CrossMark

ORIGINAL ARTICLE

Patterns of soil contamination, erosion and river loading of metals in a gold mining region of northern Mongolia

Jerker Jarsjö[1] · Sergey R. Chalov[2] · Jan Pietroń[1] · Alexey V. Alekseenko[3] · Josefin Thorslund[1]

Abstract Mining has become one of the main causes of increased heavy metal loading of river systems throughout the world. There is however an evident gap between assessments of soil contamination and metal release at the mined sites and estimates of river pollution. The present work focuses on Zaamar Goldfield, which is one of the largest placer gold mines in the world, located along the Tuul River, Mongolia, which ultimately drains into Lake Baikal, Russia. It combines field observations in the river basin with soil erosion modelling and aims at quantifying the contribution from natural erosion of metal-rich soil to observed increases in mass flows of metals along the Tuul River. Results show that the sediment delivery from the mining area to the Tuul River is considerably higher than the possible contribution from natural soil erosion. This is primarily due to excessive mining-related water use creating turbid wastewaters, disturbed filtering functions of deposition areas (natural sediment traps) close to the river and disturbances from infrastructures such as roads. Furthermore, relative to background levels, soils within Zaamar Goldfield contained elevated concentrations of As, Sr, Mn, V, Ni, Cu and Cr. The enhanced soil loss caused by mining-related activities can also explain observed, considerable increases in mass flows of metals in the Tuul River. The present example from Tuul River may provide useful new insights regarding the erosion and geomorphic evolution of mined areas, as well as the associated delivery of metals into stream networks.

Keywords Mining · Soil contamination · Erosion · Heavy metal · River contamination

✉ Jerker Jarsjö
jerker.jarsjo@natgeo.su.se

1   Department of Physical Geography, and the Bolin Centre for Climate Research, Stockholm University, SE-106 91 Stockholm, Sweden

2   Faculty of Geography, Lomonosov Moscow State University, 119991Leninskie gory, 1, Moscow, Russia

3   Faculty of Mining, Department of Geoecology, Saint Petersburg Mining University, 19910621st line V.O., 2, Saint Petersburg, Russia

Introduction

Mining has become one of the main causes of increased heavy metal loading of river systems throughout the world. There are several factors that contribute to this problem, such as (i) increased weathering rates caused by excavation and exposure of rock, (ii) leaching of metals from mine tailing impoundments (Malmström et al. 2008), (iii) erosion of waste heaps and contaminated soil from placer mining (Thorslund et al. 2012; Chalov 2014) and (iv) loading of groundwater and surface water in abandoned mine areas (Mayes et al. 2010). Mobilised metals can originate directly from exposed mine tailings or waste heaps, since mining and mineral processing operations often produce substantial quantities of solid and liquid waste. In addition, non-vegetated surface-mined lands cover significant areas in various parts of the world. It is however becoming increasingly apparent that considerable releases can also occur as a result of other disturbances at mining sites, such as altered in-channel topography or construction of roads and infrastructure (Jaramillo et al. 2015).

Heavy metal pollution from mining occurs via a variety of pathways that can be distinguished through timescales of operation and related impacts on ecosystems. Slow but sustained acid mine drainage could for instance exist as a result of

instantaneous and often catastrophic tailing dam failures. During transport, sediment-bound metals are deposited in topographic sinks located in the mining areas or at lower-lying natural flood plains and wetlands. They could then be remobilised by any type of erosive processes. The degree of river loading by metals is also influenced by in-channel storage and erosion, which underlines the complexity of contaminant dispersal, storage and remobilisation in mining areas.

Entering the fluvial system, contaminants can impact aquatic fauna and flora at an individual, community or ecosystem level. Even at sites where no heavy metals have been released, significant changes in fish communities have been reported due to riverine import of sediments impacted by mining (Lewin et al. 1977). Metal contamination also endangers human health, particularly in areas where farmlands or domestic water supplies are affected (Törnqvist et al. 2011). Inventories of pollution sources and connections between surface erosion and river processes provide a necessary basis for environmental risk assessment, mining planning and identification of mitigation measures to prevent leakage and transport of metals.

Source to recipient flows within mined areas have been studied for the last decades mostly with a focus on total sediment delivery. Experimental and modelling approaches have also addressed erosion problems of mined areas (Bartley et al. 2006; Krishnaswamy et al. 2006; Hancock et al. 2006). Fluvial system responses to sediment delivery from mines have been documented through examples of present and historical mining (Curtis et al. 2005). Recent findings from active mining areas located in Pyrenees, Spain (Martín-Vide et al. 2010), and Koryak Plateau, Russia (Chalov 2014), showed that the erosion of artificially stratified channel reaches can be a primary contributor to the annual sediment yield of mined rivers (contributing up to 40% of the total mass delivery). A few studies have aimed at obtaining a quantitative understanding of the complicated interaction between flow, sediment transport and morphological evolution in areas of sediment mining (e.g. Cao and Pender 2004; Miller 1997). However, geochemical studies on metal contamination have mostly focused on the distribution and storage in relatively small (sub)catchments (e.g. Balistrieri et al. 2007; Visser et al. 2012), which means that open questions remain regarding net effects at larger scales. There is hence an evident gap between geochemical assessments of source zones (e.g. soil contamination and metal release in mining regions; Boularbah et al. 2006; Theuring et al. 2015; Luo et al. 2010) and estimates of net impacts on recipients (e.g. river systems; Hudson-Edwards et al. 2001).

The present paper is based on extensive hydrological and geochemical field and modelling efforts considering gold-mined tributary rivers to the Selenga River, which originates in Mongolia and contributes about 50% of the total inflow into Lake Baikal. The Selenga River basin still lacks programmes for soil and water conservation. It also lacks reservoir constructions which in the global perspective cause decreased sediment fluxes (e.g. Walling and Fang 2003). At the same time, up to 35% of the catchment area in Mongolia are allocated to mining by the Mongolian government, which could transform the studied area to one of the most mining affected in the world. One of the largest placer gold mines in the world, located in the Tuul River Basin, is of particular interest since it has been reported to have a profound impact on elevated sediment-associated chemical concentrations (Chalov et al. 2015, 2016).

The present work aims at quantifying the contribution from natural erosion of metal-rich soil and waste heaps in a mining-disturbed area to observed increases in heavy metal mass flows along an intersecting river (exemplified by the Tuul River). The working hypothesis is that the contribution from soil erosion is non-negligible and quantifiable, which implies that its contribution can be compared to the observed increase that also reflects input from human disturbances in a mining area, wastewater from the mining processes, etc. We also aim at exploring potential spatial variability in heavy metal concentrations within the mining-disturbed area, investigating to which extent there are correlations with for instance land surface cover and soil type. More generally, increased knowledge on how different heavy metals are distributed in a mining-impacted landscape and the processes by which they can be transported to river systems may contribute to the identification of efficient measures for decreasing heavy metal inputs to aquatic ecosystems.

Methods

Site description

We consider the Zaamar gold mining site, which is located in the Tuul River Basin that drains into the Selenga River. The latter is the largest river of the Lake Baikal Drainage Basin (Fig. 1). The Selenga River Basin is shared between Mongolia and Russia, has an area of 477,000 km^2 and represents a relatively cold region belonging to the Arctic Ocean catchment. Average monthly temperatures range between −23.5 °C in January and 16.9 °C in July. Permafrost can be found throughout the basin, in particular in its western parts where it is continuous (Törnqvist et al. 2014). Large-scale spreading of pollutants from mining sites within the Selenga River Basin has contributed to heavy metal contamination of the Selenga River delta at Lake Baikal, which is a RAMSAR site and a UNESCO World Heritage site. More generally, the Selenga River upstream of its delta is one of the world's most impacted with regard to heavy metal loads (Viers et al. 2009; Thorslund et al. 2012).
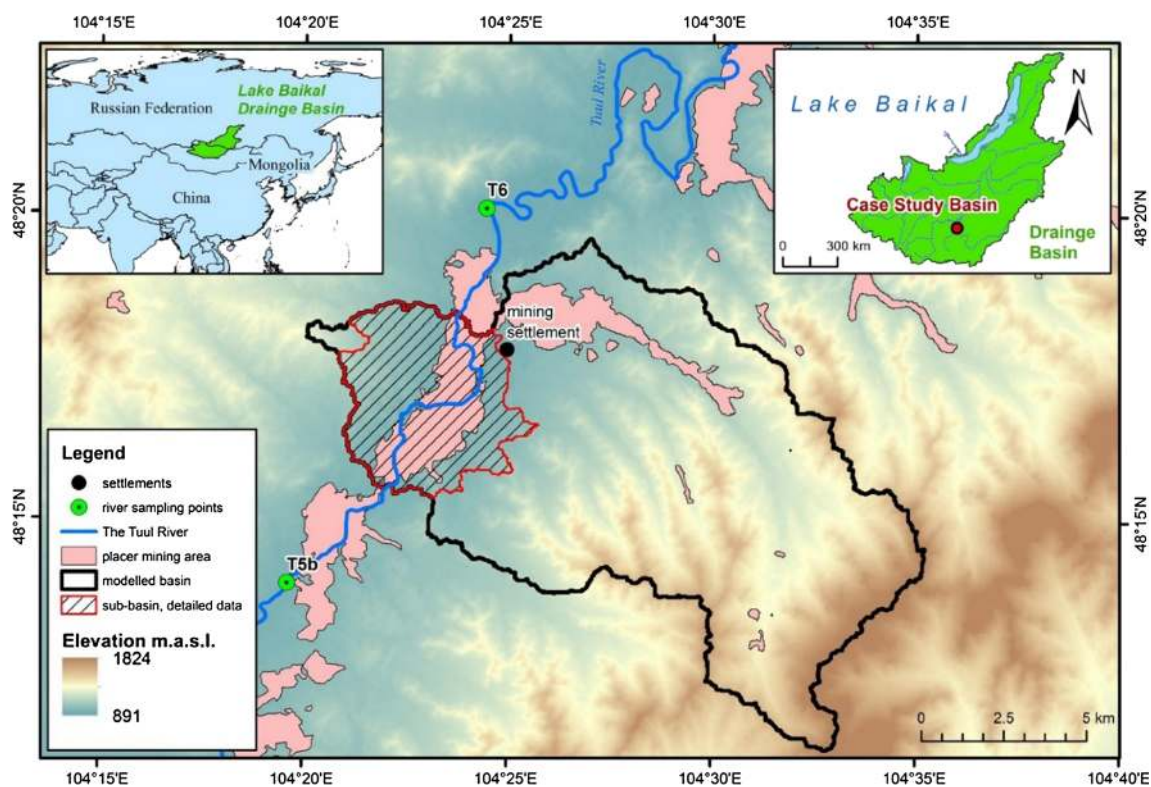
Fig. 1 Overview map showing the locations of the Lake Baikal Drainage Basin (insert map to the *left*; *grey area*) and the Zaamar case study site (insert map to the *right*; *red dot*) and modelled case study basin (*black border*) including the sub-basin (*red border*) near the Tuul River (*blue*), where detailed mapping of metal concentrations in the soil was performed. The riverine concentrations and mass flows of metals were observed at two cross sections (denoted sampling points; *filled green circle*). The areas disturbed by placer mining are marked in *pink*. Elevations range between 900 (*green*) and 1800 m (*brown*)

Placer mining of gold at Zaamar is a major enterprise in the Selenga River Basin, currently comprising around 80 mines and expanding. The middle reach of Tuul River, a tributary to the Orkhon-Selenga river system, crosses the mining site. The natural land cover in the Zaamar region mainly consists of a poorly vegetated grassland steppe. The sparse vegetation in combination with grazing makes the landscape vulnerable to erosion and degradation (MEGD 2012; Davaa and Erdenetuya 2004; Kato et al. 2009; Onda et al. 2007). The low-hill terrains and slopes are covered with chestnut soil, which is the most common soil type in the area (Qi et al. 2008). Undisturbed floodplains are covered with alluvial-sod soils (Nogina 1990); however, these have to large extent been destroyed by placer mining in the study area. The gold-bearing material is commonly extracted at depths ranging from 2 to 8 m below the top part of the alluvia (Karpoff and Roscoe 2005). As a consequence, the topographically lowest part of the catena consists of residual natural fluvisols and technosols of mining dumps (see the Electronic Supplementary Material (S1.1) for further details). Since the bedrock and soils of the region are carbonate rich, the river water contains large fractions of calcium and bicarbonates (Chalov et al. 2015), contributing to its high pH (observed to reach values above 9; Thorslund et al. 2016).

Meteorological conditions at the site are relatively dry, for instance with an average precipitation P of around 275 mm year^{-1}. The catchment area upstream of Zaamar that contributes to the flow of the Tuul River at its middle reach has an area of 55,016 km^2, within which local P values can peak at 400 mm year^{-1} in mountain regions. Most of the precipitation in the Tuul River Basin occurs during May to August, as short and intensive rainfall events (Pietroń et al. 2015). Experimental studies in grasslands near Kherlen River, east Mongolia, showed through direct erosion measurements and isotopic analyses that observed rainfall events of magnitude 7 to 15 mm/event were associated with surface runoff and erosion (Onda et al. 2007; Kato et al. 2009). The events generated sediment deliveries up to approximately 30 t km^{-2} per event. Furthermore, Theuring et al. (2013) considered the mining-affected Kharaa River Basin in Mongolia, which is a basin that neighbours the here considered Tuul River Basin. They used Be-7, Cs-137 and Pb-210 radionuclides to show that surface erosion could significantly contribute to sediment loads, at least during summer as a result of rainfall-induced discharge events.

The Tuul River has been shown to carry considerable loads of metals such as Al, As, Cu, Fe, Mn, Pb and Zn, which to large extent are attached to particles in suspension (Thorslund

et al. 2012, 2016; Chalov et al. 2012, 2015). Detailed investigations based on field measurement data from 2005, 2006, 2008, 2012 and 2013 (Thorslund et al. 2012, 2016) have shown that there are systematic trends of increasing riverine heavy metal loads over the Zaamar site, in particular over its central part (Fig. 1). However, so far, these results have not been evaluated in the context of soil contamination or erosion-deposition processes (Alekseenko and Alekseenko 2014; Pietroń et al. 2015).

Observation data

River discharge, mass flows and hydro-meteorological data

River discharge was measured and water samples were collected for chemical analysis, during two field campaigns in the Tuul River, along the Zaamar Goldfield mining site, one in June 2012 and one in September 2013 (see Thorslund et al. 2016 for more information on the site). Sample collection and discharge measurement were done simultaneously at two cross sections (T5b, *longitude 104.331, lat. 48.239* and T6, *longitude 104.420, latitude 48.239*); details on sampling procedures, laboratory analysis methods, discharge measurement methods and the calculation of dissolved and total metal mass flows are given in the Electronic Supplementary Material (S1.2).

To estimate riverine heavy metal mass flow increase (kg m^{-1} day^{-1}) over the site, the total increase in mass flow between locations T5b to T6 was divided by the total length between these locations. The distance was estimated through subdividing the river reach into five sections, connecting them with straight lines and measuring the lengths of those. The total distance was then estimated as the sum of the lengths of the straight lines. In this way, the estimated distance was unaffected by smaller-scale meandering of the river and could be seen as representative for the distance along the valley bottom.

Monthly average precipitation P, which is needed as input in the soil erosion model ("Modelling soil erosion and input of metal-contaminated sediments into the river" section) and monthly average potential evapotranspiration (E_p), was taken from the CRU dataset (Harris et al. 2014) for the months of the two field campaigns, that is, June 2012 and September 2013. However, since erosion rates and sediment concentrations in the river may vary within a month, we also estimated an adjusted P (effective precipitation P_{eff}; see the Electronic Supplementary Material S1.2) value reflecting the effective P contributing to the observed Q (Q_{obs}) This P may hence be higher or lower than the monthly average P.

For comparison, the soil erosion model was run using both monthly P (equalling 59.6 mm for June 2012 and 21.7 mm for September 2013) from CRU (Harris et al. 2014) and the field campaign-based P_{eff} (estimated at 10.2 mm for conditions of

the June 2012 campaign and 24.6 mm for conditions of the September 2013 campaign) as input. Although the 2012 measurements were conducted during a period of relatively low flows (during which $P_{eff} < P$), these alternative approaches did not affect the conclusions drawn from the respective modelling results. We also note that these 10- to 20-mm rainfall magnitudes are comparable to conditions observed in east Mongolia (Onda et al. 2007; Kato et al. 2009), during which considerable surface runoff and erosion were observed.

Soil map, soil texture and heavy metal concentration in soil

In total, 25 soil samples were taken in the upper soil horizon. Twenty of these were sampled in June 2012 along four transects perpendicular to the Tuul River, and five additional soil samples were taken in August 2014 and March 2015. Soil textural analysis was carried out as described in the Electronic Supplementary Material (S1.3). Using signature files in ArcMap 10.1, groups of representative spectral values of Landsat images (bands 1, 5 and 7) were identified. The groups were related to known soil types at the 25 soil sampling locations, and distributed over the domain using multivariate statistical analyses (maximum likelihood; see the Electronic Supplementary Material (S1.4) for further details). The resolution of the resulting map as well as the pixel resolution for all model calculations was 25 m.

Metal concentrations were determined in 20 soil samples from June 2012, which were crushed in an agate mortar and were sifted through a 0.25-mm sieve. Bulk contents of heavy metals and metalloids were analysed by mass spectrometry with inductively coupled plasma at All-Russian Research Institute of Mineral Raw Materials (Moscow), using an Elan-6100 device (PerkinElmer, USA). The sensitivity of measured concentrations was up to $1 \times 10^{-6}\%$. The resulting heavy metal concentrations were processed to create maps of their spatial variation over an area of 24 km^2 (dashed in Fig. 1) using the inverse distance weighting (IDW) method in ArcMap 10.1. Furthermore, the soil samples, which were taken in the mining region relatively close to the river, were classified as mining-disturbed in case the samples were taken from mining heaps or post-mining areas and natural if the samples were taken elsewhere. For each of the considered metals (As, Cd, Cr, Cu, Fe, Mn, Ni, Pb, Sr, V and Zn), the coefficient of variation (CV), defined as the mean value divided by the standard deviation, was calculated considering its concentration in all the 20 samples, as well as in the 10 samples of each class (mining-disturbed and natural).

Modelling soil erosion and input of metal-contaminated sediments into the river

The soil delivery from erosion in the basin (covering an area of 144 km^2; the black line of Fig. 1 shows the basin border)

was estimated using the spatially distributed, pixel-based WATEM/SEDEM model. The model was presented by Van Oost et al. (2000) and Van Rompaey et al. (2001), where its detailed description can be found; see also the Electronic Supplementary Material (S1.5) for details on how the mean soil erosion E and the transport capacity TC were calculated in the present case, as well as how the sediment routing was performed. The WATEM/SEDEM model was originally developed for Belgian loess catchments. Since then, the model and its modified version (see Verstraeten et al. 2007) have been successfully applied to semi-arid catchments characterised by silty to loamy soils and periods of intensive rainfall (Zhao et al. 2015; Haregeweyn et al. 2013; Feng et al. 2010; de Vente et al. 2008)—hence under conditions similar to those considered here. The model is sensitive to changes in soil erosion variables (e.g. land cover) and includes a sediment routing algorithm, which is important for our application. The model performance in reproducing riverine sediment loading from natural erosion was evaluated by comparison with measured increases in sediment loads along upstream reaches of the Tuul River, where there are no mining operations, although hydrogeological conditions are similar.

To estimate heavy metal mass delivery to the stream, mass erosion potentials were estimated in a first step by multiplying the metal concentrations from the created maps by the soil erosion, E. In order to identify the contribution from the areas primarily disturbed by mining and mining-related activities (Fig. 1, pink areas and the area framed by the red border), the concentrations of the heavy metals outside of these areas were set to be zero. Transport, net erosion and net deposition of heavy metals were subsequently estimated based on pixel-scale estimates of heavy metal input from erosion at upgradient areas, the local erosion and TC (Electronic Supplementary Material S1.5).

We here use a monthly time resolution, which has been found to give reasonable results in previous applications of the RUSLE model (López-Vicente et al. 2008; Diodato and Bellocchi 2007; Schiettecatte et al. 2008) and the WATEM/SEDEM model (Shi et al. 2012). Accordingly, the monthly equivalent R_m (MJ mm h^{-1} ha^{-1} $month^{-1}$) of the rainfall erosivity factor R (needed as input to calculate E) was estimated using an empirical equation proposed by Van der Knijff et al. (2000) and tested by Grimm et al. (2003) for monthly time scale $R_m = b_0 \cdot P_m$, where b_0 is an empirical coefficient (MJ h^{-1} ha^{-1}) and P_m is the monthly average precipitation (mm $month^{-1}$). We used the mean value 1.3 of the reported, reasonable b_0 range (1.1 to 1.5; Van der Knijff et al. 2000), which also has been used to represent (semi-arid) conditions in Italy (Grimm et al. 2003) and southern Europe (Van der Kniff et al. 2000). The soil erodibility factor K and normalised digital vegetation index (NDVI)-based crop/vegetation and management factor C (also needed to calculate E) were calculated according to the Electronic Supplementary Material (S1.6).

The model calculations were carried out for the 2 months of June 2012 and September 2013 to cover the time of the river discharge and in-stream heavy metal concentration measurement. The calculation of the R_m factors was then based on the estimated effective P_{eff} values. The calculation of the K factors was carried out using the map of the soil textural classes based on Landsat images from May 2013 (USGS 2014). The NDVI analyses for the C factor calculations were based on Landsat images acquired for the considered months. The maximum NDVI signals were used for defining the NDVI$_{max}$, and the values of the NDVI$_{min}$ were estimated by averaging the NDVI signals at the locations identified as bar soil during the campaign in June 2012. The delineation of the modelled basin area and the estimation of all topographic parameters (e.g. slope gradient and LS$_{2D}$ factor) were carried out using the ASTER digital elevation model (DEM; USGS 2014), with a 1″ resolution of the acquired raw DEM (corresponding to about 30 m horizontal and 20 m vertical resolution at N48E104). The data was processed in ArcMap 10.1 to remove sinks and imperfections from the DEM and to adjust the location of the Tuul River in the model.

Results

Observed total mass transport of sediment and metals in the river at the mining area

During the measurement campaign of June 2012, the observed total sediment load of Tuul River was 67 t day^{-1} at location T5b in the upstream part of the mining area. The sediment load increased to a value of 143 t day^{-1} at T6, located 13 km downstream of T5b, implying a sediment load increase per unit river length of 5.9 kg m^{-1} day^{-1}. This value represents an average increase over the mining area and is much higher than the average increase upstream of the mining area of 0.13 kg m^{-1} day^{-1} (also observed in June 2012). The river discharge was similar at T5b and T6 (12.4 and 12.2 m^3 s^{-1}, respectively). In 2013, the river discharge was considerably higher (35.3 and 44.9 m^3 s^{-1}, respectively), resulting in about twice as high sediment loads and load increases.

Table 1 presents absolute, average mass flow values of metals at location T5b in the upstream part of the mining area and location T6 in the downstream part (Fig. 1) for the measurement campaigns of June 2012 and September 2013. Table 1 also shows the corresponding increases in mass flow per river length unit (m), which can reflect metal inputs along the river. In 2012, which also is the year of mapping metal concentrations in the soil (see "Observed metal concentrations in soil" section), Fe, Mn, Zn, V and Cr show the overall highest increases over the mining site, with values ranging between 2.2×10^{-4} (Cr) and 0.17 (Fe) kg per day per metre river. Most of these metals also show relatively high absolute

Table 1 Observed average riverine mass flows (kg day^{-1}) for each metal, sample year (2012 and 2013) and location (T5b and T6), as well as corresponding mass flow increase per metre river (kg m^{-1} day^{-1}) between T5b and T6

	As	Cd	Cr	Cu	Fe	Mn	Ni	Pb	Sr	V	Zn
2012											
Mass flow at T5b (kg day^{-1})	20.1	1.20	2.42	0.13	986	203	5.62	3.71	294	9.69	9.56
Mass flow at T6 (kg day^{-1})	15.7	1.17	5.47	1.92	3350	246	7.33	6.63	270	13.6	18.1
Mass flow increase per metre river (kg m^{-1} day^{-1})	-3.11×10^{-4}	-2.28×10^{-6}	2.18×10^{-4}	1.28×10^{-4}	1.69×10^{-1}	3.03×10^{-3}	1.32×10^{-4}	2.08×10^{-4}	-1.72×10^{-3}	2.82×10^{-4}	6.13×10^{-4}
2013											
Mass flow at T5b (kg day^{-1})	5.43	0.07	17.0	3.57	2450	146	2.63	5.09	698	9.76	63.4
Mass flow at T6 (kg day^{-1})	13.9	0.03	18.7	4.01	4220	229	5.16	7.37	885	16.6	104
Mass flow increase per metre river (kg m^{-1} day^{-1})	6.06×10^{-4}	-2.77×10^{-6}	1.19×10^{-4}	3.15×10^{-5}	1.26×10^{-1}	5.97×10^{-3}	1.95×10^{-4}	1.63×10^{-4}	1.34×10^{-2}	4.91×10^{-4}	2.91×10^{-3}

mass flow values at T5b, that is, at the upstream end of the site (Fe, Mn, Zn and V; ranging between 9.6 kg day^{-1} for Zn and 986 kg day^{-1} for Fe). Other metals (As, Cd and Zn) show no accumulation or a slightly decreasing trend over the mining site. For 2013, the trends are similar, except that Sr shows high mass flow increase (in addition to Fe, Mn, Zn and V as in 2012), and also, As shows a non-negligible trend of accumulation.

Results in terms of normalised increases, where the mass flow increase between locations T5b and T6 is expressed in percent of the mass flow at the upstream T5b location, is shown in Fig. 2. The figure for instance illustrates that there are high relative increases of Cu (1360%; outside of axis range), Fe (240%) and Cr (125%), indicating that input from the mining region alter their riverine mass flows most of all considered metals. However for Cu, in contrast to Fe and Cr, this high increase is relative to a very low absolute mass in-flow to the mining site.

Soil map, slope angles, vegetation and soil erosion modelling results

The distribution of the five soil textural classes identified in the studied area (Fig. 3) shows that relatively fine soils (sandy loam in green and loam in yellow) are located along Tuul River and within the mining areas. These are richer in silts than the loamy sands (red) that dominate in the upper parts of the basin. The topography of the areas close to the Tuul River are characterised by gentler slopes (0–5°), in contrast to the middle and upper parts of the basin that contain mountain sides with slopes of up to 50°. Vegetation is essentially absent in the regions most disturbed by mining and roads, as reflected in a C-factor ("Modelling soil erosion and input of metal-contaminated sediments into the river" section and Electronic Supplementary Material S1.5) close to 1 in the vicinity of the Tuul River and in the northern part of the basin (Fig. 3).

Figure 4 shows erosion and deposition patterns according to the soil erosion model, indicating that many flat areas in the vicinity of Tuul River are dominated by net deposition (green). Such areas are frequently bordered by areas of low erosion. However, notably, there are also considerable patches in the vicinity of Tuul River that have moderate to high erosion. This is related to the fact that soils are fine grained and vegetation is sparse due to mining activities and traffic on dirt roads (see the vegetation factor in Fig. 3), which enhances erosion even in such relatively flat areas. Furthermore, erosion was predicted to be considerably higher in September 2013 than in June 2012, because the precipitation, used as input to the model, is higher in the former case.

Regarding the net input of sediments into the Tuul River, resulting from the erosion and deposition patterns from hill-slope processes shown in Fig. 4, the contribution was

Fig. 2 Relative increase in mass flow (%) of each metal between the two sampled locations (T5b and T6). The difference in mass flow between the two locations are normalised by the absolute value of T5b. The *solid line* corresponds to sampling in 2012, and the *dashed line* corresponds to sampling in 2013
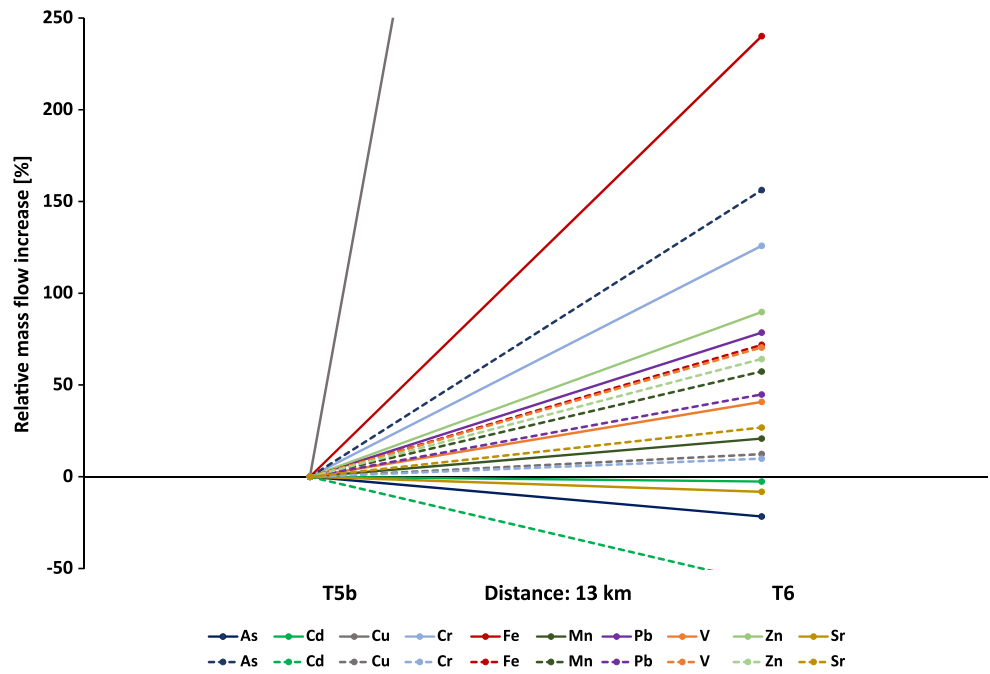

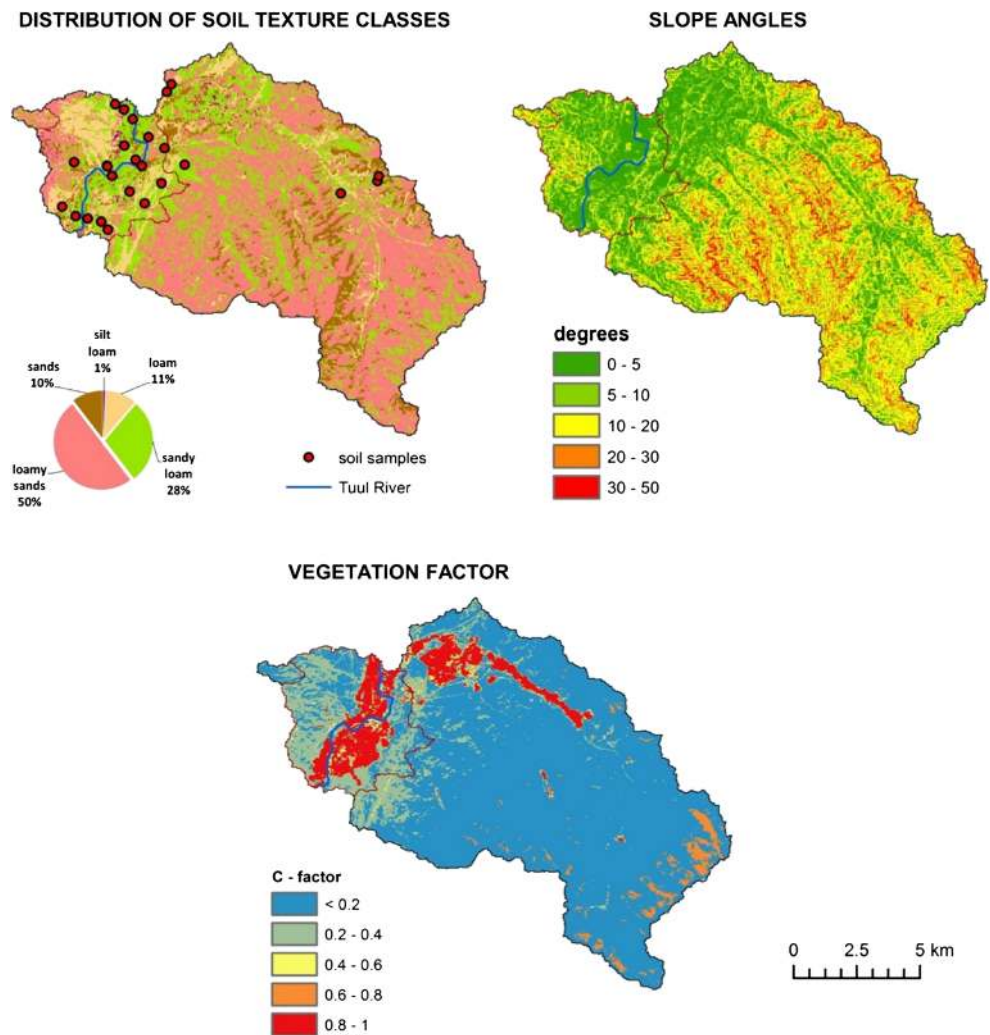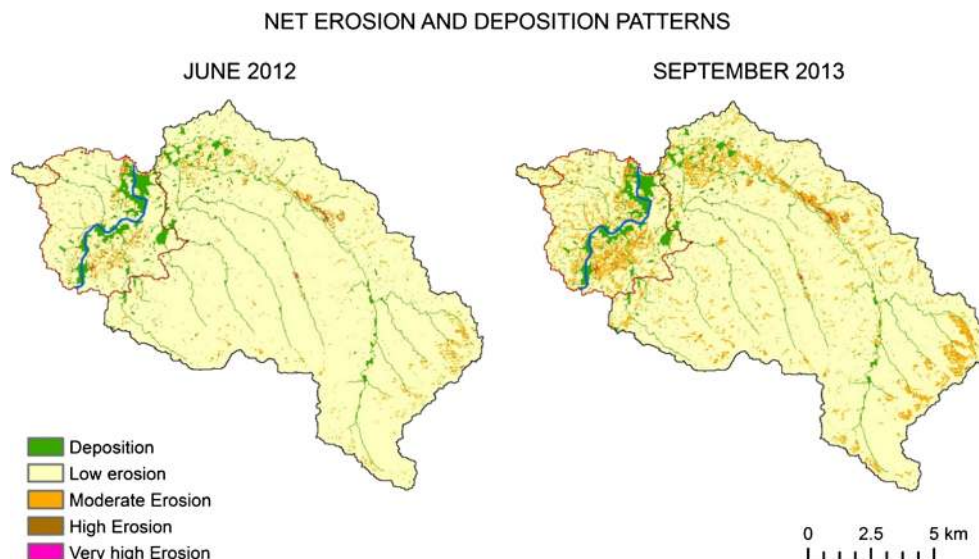**Fig. 3** Soil map, slope angles and vegetation factor

Fig. 4 Modelled net erosion and deposition patterns: very high erosion (>8 kg m^{-2} month^{-1}), high erosion (4–8 kg m^{-2} month^{-1}), moderate erosion (2–4 kg m^{-2} month^{-1}), low erosion (0–2 kg m^{-2} month^{-1}) and net deposition

predicted to be 28 t month^{-1} for June 2012 and 59 t month^{-1} for September 2013. This corresponds to specific (net) erosion rates of 0.20 and 0.42 t month^{-1} km^{-2}, respectively, and sediment load increases along the Tuul River of 0.16 kg m^{-1} day^{-1} in 2012 and 0.33 kg m^{-1} day^{-1} in 2013.

Observed metal concentrations in soil

Figure 5 shows absolute concentrations of As, Fe, Zn, Pb, Sr, Cd, Mn, V, Ni, Cu and Cr in mining areas around the Tuul River, measured in 2012. For many metals, the highest observed concentrations are about twice as high as the lowest ones. A lower range than that is shown by Cd (0.17 to 0.24 mg kg^{-1}), which contrasts to the relatively high As range (8 to 31 mg kg^{-1}). Overall, considering metal concentrations of all 20 measurement points, the coefficient of variation (CV) was modest with a median value of 19%. However, although mining activities occur in the entire region depicted in Fig. 5, local soil conditions range from natural to heavily mining disturbed. Considering the 10 measurement points taken in naturally occurring soils furthest away from the mined river, the CV was considerably lower for all metals except Pb and Mn, with a median value of 8%. In Fig. 5, this is reflected in relatively uniform concentration fields to the far left and far right of the river and a patchiness in metal concentrations close to the river. Notably, if there would have been more measurement points close to the river, the map interpolation would most likely have shown even larger patchiness there.

There are certain sampling points that consistently have high metal concentrations. For instance, the concentration is equal to or near its maximum observed value for As, Fe, Zn, V, Ni, Cu and Cr in a sampling point in the middle-left part of the figures (where the Tuul River makes a pronounced, 180° turn to the left; the flow direction is from south to north). Furthermore, the sampling point to the south, on the other side

of the river, also shows high concentrations of many metals, including Fe, Zn, V, Ni, Cu and Cr. Both these points are located in the flattest part of the basin, which is dominated by sandy loams and loams. Pb has a different pattern, showing high concentrations in the top-right part of the basin, where the mining settlement is located. Such elevation of Pb values in urban areas are well documented in many regions (Goldhaber et al. 2009), where they have been explained by fuelling of vehicles with leaded gasoline and use of paint containing Pb. In particular, Kasimov et al. (2011) investigated the issue of soil pollution with Pb in Ulaanbaatar, showing that the main source is leaded gasoline that is not prohibited in Mongolia. This problem is hence likely shared with the villages of the Zaamar area and the rest of the Tuul Basin.

Results regarding the possible relations between soil texture class (Fig. 3) and soil metal concentration (Fig. 5) show diverging patterns. Five of the considered 11 metals show increasing average concentrations in soils with finer texture. The most pronounced trend is found for Zn that shows an average concentration in sand of 52 mg kg^{-1}, which increases for finer soil textures, up to 75 mg kg^{-1} in silt loam. Also, Ni shows a clear trend, increasing from 25 mg kg^{-1} in sand to 34 mg kg^{-1} in silt loam. Increasing trends for finer textures are also found for Cd (0.16 to 0.23 mg kg^{-1}), Cu (22 to 30 mg kg^{-1}) and Sr (300 to 390 mg kg^{-1}). In contrast, the average As concentration in sand of 15 mg kg^{-1} decreases gradually for finer soil texture down to 13 mg kg^{-1} in silt loam. The remaining five metals (Cr, Pb, V, Fe, Mn) show no clear relation between concentration in soil and soil texture.

Modelled heavy metal input to the river due to erosion of contaminated soil

Taking into account the observed metal concentrations in soil (Fig. 5), the spatially distributed erosion rates (Fig. 4) and the
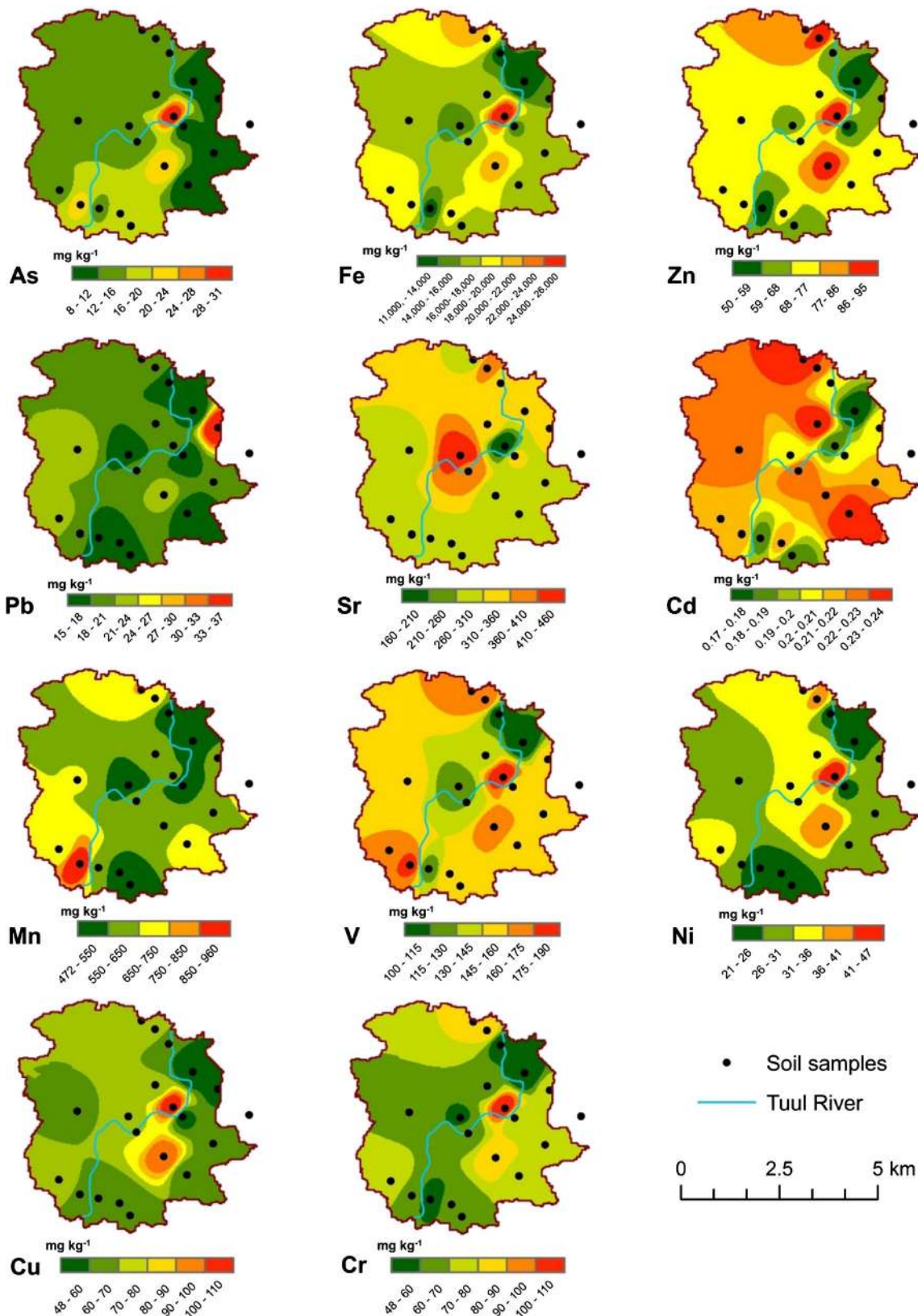
Fig. 5 Concentration of metals in soil in the mining-disturbed region around Tuul River

associated net input of eroded and metal-contaminated soil into the Tuul River ("Soil map, slope angles, vegetation and

soil erosion modelling results" section), Table 2 shows the estimated total mass delivery of heavy metals to the river

due to soil erosion in June 2012 and September 2013. For instance, in 2012, values range from 3 g month^{-1} of Cd to 211 kg month^{-1} of Fe. In order to make these estimated erosion-related metal deliveries comparable to the observed increases over the mining site of mass flows of metals in the river (Table 1), Table 2 also shows the average delivery of metals per day and metre river length, yielding values between 1.4×10^{-8} kg m^{-1} day^{-1} for Cd and 1.2×10^{-3} kg m^{-1} day^{-1} for Fe. Specifically, Table 2 shows that Fe, Mn, Sr, V and Cr are estimated to have the highest mass deliveries due to soil erosion, whilst As, Cd and Pb are estimated to have low erosion-related deliveries. A comparison of these estimated soil erosion-related deliveries and the observed mass flow increases of metals in the Tuul River along the mining region is made in the "Discussion" section.

Discussion

Estimated soil erosion and observed riverine sediment load increases

In comparison with the estimated contribution from natural soil erosion to the sediment loading of Tuul River in June 2012 of 0.16 kg per metre river per day ("Soil map, slope angles, vegetation and soil erosion modelling results" section), the observed increase between points T5b and T6 was much greater, 5.9 kg per metre river per day ("Observed total mass transport of sediment and metals in the river at the mining area" section). This order-of-magnitude difference is too large to be explained by measurement errors, or errors from methodological simplifications, such as possibly unaccounted for contributions from natural erosion of the riverbanks (Hartwig et al. 2016). This implies that the relative contribution of natural erosion to the observed increases in riverine sediment load is limited within the mining area. We note that finer soils contributed more to the sediment load in the river over the mining area than upstream of it.

The model performance in reproducing sediment loading from natural erosion can be evaluated by comparison with the observed average increase of sediment load along the entire Tuul River reach upstream of the mining area, which was 0.13 kg m^{-1} day^{-1}. This is hence very close to the modelled contribution from natural hillslope erosion. This result is consistent with the model evaluation results of Pietroń et al. (2017), who considered the erosion and soil loss of a relatively large region (1680 km^2) around Zaamar Goldfield using the same basic model setup as we do. More specifically, they found that their model results on natural erosion agreed with observed river loading from erosion of natural areas located between the mining regions (in nested catchments).

The above-mentioned contribution of (natural) soil erosion of 0.16 kg m^{-1} day^{-1} to Tuul River was observed in June 2012

Table 2 Estimated mass delivery from soil erosion (kg day^{-1}) from the modelled sub-basin for each metal and sample year (2012 and 2013) as well as corresponding mass flow increase per metre river (kg m^{-1} day^{-1}) between T5b and T6

	As	Cd	Cr	Cu	Fe	Mn	Ni	Pb	Sr	V	Zn
2012											
Delivery to the river from soil erosion (kg month^{-1})	0.18	0.003	0.86	0.33	211	7.27	0.37	0.23	3.91	1.77	0.87
Delivery per metre river (kg m^{-1} day^{-1})	1.03×10^{-6}	1.43×10^{-8}	4.78×10^{-6}	1.87×10^{-6}	1.18×10^{-3}	4.06×10^{-5}	2.08×10^{-6}	1.29×10^{-6}	2.18×10^{-5}	9.88×10^{-6}	4.86×10^{-6}
2013											
Delivery to the river from soil erosion (kg month^{-1})	0.09	0.001	0.41	0.16	100	3.47	0.18	0.11	1.86	0.84	0.41
Delivery per metre river (kg m^{-1} day^{-1})	4.88×10^{-7}	6.84×10^{-9}	2.27×10^{-6}	8.86×10^{-7}	5.60×10^{-4}	1.94×10^{-5}	9.88×10^{-7}	6.11×10^{-7}	1.04×10^{-5}	4.70×10^{-6}	2.31×10^{-6}

and corresponds to an area-averaged specific erosion of 0.20 t month^{-1} km^{-2}. In September 2013, when the discharge of Tuul River was about three times the one of June 2012, the area-averaged erosion was estimated at 0.42 t month^{-1} km^{-2}. This range is for instance consistent with observed conditions in semi-arid rangelands in North Queensland, Australia (Bartley et al. 2006). Specifically, two of their three experimental sites in Bartley et al. (2006) had similar runoff to rainfall ratios as in this study (<0.1; as well as similar average P of around 235 mm year^{-1}) and showed average soil erosion rates between 0.29 and 1.20 t month^{-1} km^{-2}. However, their values represent annual averages, whereas we here present estimates relevant on a monthly timescale (or slightly shorter). In particular, intense precipitation events and associated flow peaks can have relatively pronounced effect on sediment delivery. Chalov et al. (2015) and Pietroń et al. (2015) investigated inter-annual variability of the here considered Tuul River in detail, showing that around 70% of the annual sediment transport occur during peak flow events that have a duration of 2.4 months (20% of a year). The here considered discharge of 12 m^3 s^{-1} in June 2012 is classified as base-flow conditions in Chalov et al. (2015), and the discharge of around 40 m^3 s^{-1} in September 2013 is classified as peak flow conditions in Chalov et al. (2015), which shows that both conditions are represented in the present analyses.

As also noted above, the contribution of soil erosion is small relative to observation-based estimates of total sediment load increase per unit river length across the mining area of 5.9 kg m^{-1} day^{-1}, which in terms of equivalent input normalised from contributing land area corresponds to a soil loss of 8.45 t month^{-1} km^{-2}. Similar or even higher rates of soil loss have been attributed to soil erosion in regions where precipitation is higher than in the Tuul River Basin, such as in the Mae Tao Basin in Thailand (Somprasong and Chaiwiwatworakul 2015) and in the Maracas-Saint Joseph River Basin in Trinidad and Tobago (Jaramillo et al. 2015). A remaining plausible explanation for the considerably elevated rates of soil loss in the arid Tuul River Basin is that the loss is directly related to the excessive mining-related water use and water circulation, which is also supported by recent results of Pietroń et al. (2017) who studied a series of nested catchments in the region. Furthermore, observations on the Zaamar mining site (August 2015) show that even during dry conditions, a contributing stream discharging into Tuul River was highly turbid (445 NTU) with large variability in discharge, which can reflect contributions from process water that is pumped from the river to the adjacent mining area. Similar water turbidity in streams has been reported for areas affected by surface mining (e.g. 424–2874 NTU in Gros Rosebel gold mining area in Suriname; Mol and Ouboter 2004).

Furthermore, regions with intense placer mining (pink areas in Fig. 1) overlap with regions where deposition of eroded soils naturally occur (green areas in Fig. 4). Under undisturbed conditions, such deposition areas may hence function as natural filters, limiting the net erosion and input of eroded material into stream networks. However, under conditions of mining disturbance, such fresh deposits transported from higher elevations through natural erosion processes may be remobilised together with the excavated sediments. Taken together, this indicates that the sediment delivery to the river from the mining area is considerably enhanced over natural levels due to soil erosion from excessive mining-related water use, disturbed natural sediment filtering functions of deposition areas close to the river and soil loss related to other physical disturbances from mining operations and infrastructure such as roads.

In principle, in-channel processes could also result in considerable sediment load changes along rivers. For example, results of Pietroń et al. (2015) for the here considered Tuul River imply that such processes in an alternate manner can shift between reinforcing to counteracting input signals from processes in the catchment itself. However, the here reported sediment load increases over the Zaamar mining area have consistently been seen in repeated observations under different hydrological conditions and at different times (Thorslund et al. 2012, 2016; Chalov et al. 2012, 2015; Pietroń et al. 2015), which suggests that the signal from this mining-disturbed part of the catchment appears sufficiently high in relation to the potential noise from in-channel processes of the river.

Soil metal concentrations, metal delivery from soil erosion and riverine metal load increases

For several metals, the absolute concentrations in soil (Fig. 5) are relatively high in comparison with the background conditions. For instance, the concentrations of Zn, Ni and Sr are up to 2.8 higher in the considered mining-disturbed soil cover than under undisturbed conditions. Furthermore, in comparison with extensive datasets on background levels, derived from approximately 1000 topsoil samples each (summarised in Goldhaber et al. 2009), including Europe (Salminen et al. 2005) and North America (Shacklette and Boerngen 1984; Gustavsson et al. 2001), the soils of the here considered Zaamar mining region contain higher concentrations of As (Zaamar median 13 mg kg^{-1}; compared to the median values of 7.0 and 5.8 mg kg^{-1} of the European and American studies, respectively), Sr (305 mg kg^{-1}; compared to 89 and 150 mg kg^{-1}), Mn (589 mg kg^{-1}; compared to 503 and 300 mg kg^{-1}), V (150 mg kg^{-1}; compared to 60 and 70 mg kg^{-1}), Ni (28 mg kg^{-1}; compared to 18 and 15 mg kg^{-1}), Cu (25 mg kg^{-1}; compared to 13 and 20 mg kg^{-1}) and Cr (69 mg kg^{-1}; compared to 60 and 50 mg kg^{-1}). Furthermore, Goldhaber et al. (2009) reports results from a region of 20,000 km^2 around the Sacramento River Basin, which

contains a mixture of urban and agricultural regions that are clearly impacted by mining of mercury and gold, including disturbances from regions of placer mining. Interestingly, Goldhaber et al. (2009) report elevated values above background levels of a similar set of metals and to a similar extent as found here, including Sr (reporting a median value of 226 mg kg^{-1}), Mn (752 mg kg^{-1}), V (135 mg kg^{-1}), Ni (50 mg kg^{-1}), Cu (37 mg kg^{-1}) and Cr (96 mg kg^{-1}). In the Zaamar region, concentrations of As and V occur at ecologically hazardous levels, exceeding maximum permissible levels established in Mongolia for loamy soil (Dorzhgotov and Bathishig 2008). The local As concentrations were on the average about four times higher than the state-permitted level, up to nine times in several points. However, it should be noted that even in undisturbed areas of the Zaamar region, a twofold excess was noted. The Mongolian maximum permissible levels for As were hence established without considering the regional geochemical characteristics of soils and rocks enriched with the element (see also Kasimov et al. 2011).

The observed increases in riverine mass flows of metals over the mining site were much higher than what could be explained by the contribution from natural erosion of exposed, metal contaminated soil within the mining area. For instance, Fe and Cr were observed to increase with 0.17 and 2.2×10^{-4} kg per day per metre river, respectively ("Observed total mass transport of sediment and metals in the river at the mining area" section). This is orders of magnitude higher than the estimated contribution from erosion of contaminated soil, which was 1.2×10^{-3} and 5.6×10^{-6} kg per day per metre river for Fe and Cr, respectively ("Modelled heavy metal input to the river due to erosion of contaminated soil" section). Since both the estimated riverine mass flows and the soil contamination data are associated with uncertainties related to spatiotemporal variability, we checked to which extent these could influence present results. As mentioned earlier in the "Results" section, considering metal concentrations of all 20 measurement points in soil, the median CV was 19%. Furthermore, regarding the riverine mass flows (Table 1), the (monthly) CV was estimated in Thorslund et al. (2012) based on previous, extensive measurements (15 field campaigns, each comprising repeated concentration and discharge measurements) from the Zaamar area. The results showed a median CV of 35%. Notably, our conclusions regard the difference between the metal input flux from soil erosion and the total mass flux of metals in the river, which was at least 100 times larger than even the highest of these CV values (e.g. 3900% for Cr and 14,200% for Fe). The conclusion regarding the total mass flux of metals in the river being much larger than the soil erosion contribution therefore appears to be robust. This hence shows that natural erosion of contaminated soil has small impact on metal loads observed in the river. This is partly because the total amount of material entering the river by natural erosion is being overshadowed by the amount of sediment that enters the river in other ways, for instance through effluent waters of mining.

Notably, the relative abundance of different metals found in the soil within the mining area reflects very well the relative abundance of metals found in suspended sediments of the Tuul River. For instance, in the Tuul River at the mining site, the highest total longitudinal increase of riverine metal concentrations were found for Fe, Mn, Zn, V and Cr. In the soil of the mining area, the highest total metal concentrations were found for Fe, Mn, Sr, V and Cr. Furthermore, As, Cd and Zn were not enriched in the river in 2012, which agrees relatively well with the lowest absolute soil concentrations being As, Cd and Pb (note however that due to the toxicity of As, these absolute concentrations are still of concern and can be considered to be high from a health perspective). This shows that metals found in the river are likely to be related to surface soils of the mining area and its vicinity, although the transport must have occurred through other processes than natural erosion.

The present example from Tuul River may provide useful new insights regarding the erosion and geomorphic evolution of mined areas, as well as the associated delivery of metals into stream networks. These matters should be addressed in key environmental actions such as mine closure plans and land reclamation projects. For instance, present results suggest that relevant measures in Zaamar Goldfield include construction and proper management of settling ponds, which can absorb the identified high amounts of metal-contaminated sediments that are eroded by excess water from mining operations. Waste material and existing settling ponds are however mismanaged in the Zaamar Goldfield, which leads to high discharge of fine material into the Tuul River (e.g. Farrington 2000). Further improvement may be achieved by restoration of waste deposits through landform design, involving the creation of stable mature landscapes, which can withstand erosion much more easily. The present study emphasises that this may also be important in identified zones of natural deposition, since such actions could restore natural sediment filtering functions of the landscape, which prevent material from being further transported into the river network.

Conclusions

The soil erosion rate within Zaamar Goldfield, Mongolia, is high considering the arid conditions, showing values on the order of 10 t month^{-1} km^{-2}. The associated sediment delivery from the mining area to Tuul River, which intersects the Zaamar Goldfield, is estimated to be considerably higher than the possible contribution from natural soil erosion. Results suggest that this high delivery of sediments into the Tuul River primarily can be explained by excessive mining-related water use creating turbid wastewaters, disturbed

natural sediment filtering functions in deposition areas close to the river and disturbances from mining operations and infrastructure such as roads.

Relative to background levels, soils within Zaamar Goldfield contain elevated concentrations of As, Sr, Mn, V, Ni, Cu and Cr. This is consistent with findings from a placer mining-impacted area in Northern California. Concentrations of As and V occur at ecologically hazardous levels. Five of the considered 11 metals showed increasing average concentrations in soils with finer soil texture (Zn, Ni, Cd, Cu and Sr). The enhanced soil loss caused by mining-related water use and mining operations can also explain the observed, considerable increases in mass flows of metals in the Tuul River. Specifically, these observed increases were much higher than could be explained by the contribution from natural erosion of exposed, metal-contaminated soil within the mining area. The present example from Tuul River may provide useful new insights regarding the erosion and geomorphic evolution of mined areas, as well as the associated delivery of metals into stream networks. These matters should be addressed in key environmental actions such as mine closure plans and land reclamation projects.

References

Alekseenko V, Alekseenko A (2014) The abundances of chemical elements in urban soils. J Geochem Explor 147(B):245–249. doi:10.1016/j.gexplo.2014.08.003

Bartley R, Roth CH, Ludwig J, McJannet D, Liedloff A, Corfield J, Hawdon A, Abbott B (2006) Runoff and erosion from Australia's tropical semi-arid rangelands: influence of ground cover for differing space and time scales. Hydrol Process 20:3317–3333. doi:10.1002/hyp.6334

Balistrieri LS, Seal RR, Piatak NM, Paul B (2007) Assessing the concentration, speciation, and toxicity of dissolved metals during mixing of acid-mine drainage and ambient river water downstream of the Elizabeth copper mine, Vermont, USA. Appl Geochem 22(5):930–952. doi:10.1016/j.apgeochem.2007.02.005

Boularbah A, Schwartz C, Bitton G, Morel JL (2006) Heavy metal contamination from mining sites in South Morocco: 1. Use of a biotest to assess metal toxicity of tailings and soils. Chemosphere 63:802–810. doi:10.1016/j.chemosphere.2005.07.079

Cao Z, Pender G (2004) Numerical modelling of alluvial rivers subject to interactive sediment mining and feeding. Adv Water Resour 27:533–546. doi:10.1016/j.advwatres.2004.02.017

Chalov SR, Zavadsky AS, Belozerova EV, Bulacheva MP, Jarsjö J, Thorslund J, Yamkhin J (2012) Suspended and dissolved matter fluxes in the upper Selenga River Basin. Geography Environment Sustainability 5(2):78–94. doi:10.24057/2071-9388-2012-5-2-78-94

Chalov SR (2014) Effects of placer mining on suspended sediment budget: case study of north of Russia's Kamchatka peninsula. Hydrolog Sci J 59(5):1081–1094. doi:10.1080/02626667.2014.903330

Chalov SR, Jarsjö J, Kasimov NS, Romanchenko AO, Pietroń J, Thorslund J, Promakhova EV (2015) Spatio-temporal variation of sediment transport in the Selenga River Basin, Mongolia and Russia. Environ Earth Sci 73:663–680. doi:10.1007/s12665-014-3106-z

Chalov SR, Thorslund J, Kasimov N, Aybullatov D, Ilyicheva E, Karthe D, Kositsky A, Lychagin M, Nittrouer J, Pavlov M, Pietroń J, Shinkareva G, Tarasov M, Garmaev E, Akhtman Y, Jarsjö J (2016) The Selenga River delta—a geochemical barrier protecting Lake Baikal waters. Reg Environ Change (this issue). doi:10.1007/s10113-016-0996-1

Curtis JA, Flint LE, Alpers CN, Yarnell SM (2005) Conceptual model of sediment processes in the upper Yuba River watershed, Sierra Nevada, CA. Geomorphology 68:149–166. doi:10.1016/j.geomorph.2004.11.019

Davaa G, Erdenetuya M (2004) Hydrological changes in the upper Tuul River Basin . In: Proceedings of the 3rd International Workshop on Terrestrial Change in Mongolia, Tsukuba, Japan, pp. 16–19

de Vente J, Poesen J, Verstraeten G, Van Rompaey A, Govers G (2008) Spatially distributed modelling of soil erosion and sediment yield at regional scales in Spain. Glob Planet Chang 60(3):393–415. doi:10.1016/j.gloplacha.2007.05.002

Diodato N, Bellocchi G (2007) Estimating monthly (R)USLE climate input in a Mediterranean region using limited data. J Hydrol 345(3):224–236. doi:10.1016/j.jhydrol.2007.08.008

Dorzhgotov D, Bathishig O (2008) Хрсний чанар. Хрс бохирдуулагч бодис, элемент дийн звш ргдх дээд хэмжээ. Монгол улсын стандарт. Standartchilal, hemzhilz yn ndesny t v, Ulaanbaatar, pp. 8 (in Mongolian).

Farrington J (2000) Environmental problems of placer gold mining in the Zaamar Goldfield, Mongolia. World Placer Journal 1:107–128, available electronically at http://bic.iwlearn.org/mn/

Feng X, Wang Y, Chen L, Fu B, Bai G (2010) Modeling soil erosion and its response to land-use change in hilly catchments of the Chinese loess plateau. Geomorphology 118(3):239–248. doi:10.1016/j.geomorph.2010.01.004

Grimm M, Jones RJA, Rusco E, Montanarella L (2003) Soil erosion risk in Italy: a revised USLE approach. EUR 20677 EN, Office for Official Publications of the European Communities, Luxemburg, Luxemburg, pp. 26

Goldhaber MB, Morrison JM, Holloway JM, Want RB, Helsel DR, Smith DB (2009) A regional soil and sediment geochemical study in Northern California. Appl Geochem 24(8):1482–1499. doi:10.1016/j.apgeochem.2009.04.018

Gustavsson N, Bølviken B, Smith DB, Severson RC (2001) Geochemical landscapes of the conterminous United States: new map presentations for 22 elements. US Geol Surv Prof Paper 1648. <http://www.pubs.usgs.gov/pp/p1648/>

Hancock GR, Grabham MK, Martin P, Evans KG, Bollhöfer A (2006) A methodology for the assessment of rehabilitation success of post mining landscapes—sediment and radionuclide transport at the

former Nabarlek uranium mine, Northern Territory, Australia. Sci Total Environ 354:103–119. doi:10.1016/j.scitotenv.2005.01.039

Harris I, Jones PD, Osborn TJ, Lister DH (2014) Updated high resolution grids of monthly climatic observations—the CRU TS3. 10 dataset. Int J Climatol 34(3):623–642. doi:10.1002/joc.3711

Haregeweyn N, Poesen J, Verstraeten G, Govers G, de Vente J, Nyssen J, Deckers J, Moeyersons J (2013) Assessing the performance of a spatially distributed soil erosion and sediment delivery model (WATEM/SEDEM) in northern Ethiopia. Land Degrad Dev 24(2):188–204. doi:10.1002/ldr.1121

Hartwig M, Schäffer M, Theuring P, Avlyush S, Rode M, Borchardt D (2016) Cause–effect–response chains linking source identification of eroded sediments, loss of aquatic ecosystem integrity and management options in a steppe river catchment (Kharaa, Mongolia). Environ Earth Sci 75(10):1–13. doi:10.1007/s12665-015-5092-1

Hudson-Edwards KA, Macklin MG, Miller JR, Lechler PJ (2001) Sources, distribution and storage of heavy metals in the Rio Pilcomayo, Bolivia. J Geochemical Explor 72:229–250. doi:10.1016/S0375-6742(01)00164-9

Jaramillo F, Baccard M, Narinesingh P, Gaskin S, Cooper V (2015) Assessing the role of a limestone quarry as sediment source in a developing tropical catchment. Land Degrad Dev 27(4):1064–1074. doi:10.1002/ldr.2347

Karpoff, BS, Roscoe, WE (2005) Report on placer gold properties in the Tuul Valley, Zaamar Goldfield, Mongolia. Roscoe Postle Associates Inc, Toronto, Canada

Kasimov NS, Kosheleva NE, Sorokina OI, Bazha SN, Gunin PD, Enkh-Amgalan S (2011) Ecological-geochemical state of soils in Ulaanbaatar (Mongolia). Eurasian Soil Sci 44(7):709–721. doi:10.1134/S106422931107009X

Kato H, Onda Y, Tanaka Y, Asano M (2009) Field measurement of infiltration rate using an oscillating nozzle rainfall simulator in the cold, semiarid grassland of Mongolia. Catena 76(3):173–181. doi:10.1016/j.catena.2008.11.003

Krishnaswamy J, Bunyan M, Mehta VK, Jani N, Karanth KU (2006) Impact of iron ore mining on suspended sediment response in a tropical catchment in Kudremukh, western Ghats, India. Forest Ecol Manag 224:187–198. doi:10.1016/j.foreco.2005.12.018

Lewin J, Davies BE, Wolfenden PJ (1977) Interactions between channel change and historic mining sediments. In: Gregory KJ (ed) River channel changes. Wiley, Chichester, pp 353–367

López-Vicente M, Navas A, Machín J (2008) Identifying erosive periods by using RUSLE factors in mountain fields of the central Spanish Pyrenees. Hydrol Earth Syst Sci 12(2):523–535. doi:10.5194/hess-12-523-2008

Luo W, Lu Y, Zhang Y, Fu W, Wang B, Jiao W, Wang G, Tong X, Giesy JP (2010) Watershed-scale assessment of arsenic and metal contamination in the surface soils surrounding Miyun reservoir, Beijing, China. J Environ Manag 91:2599–2607. doi:10.1016/j.jenvman.2010.07.023

Malmström ME, Berglund S, Jarsjö J (2008) Combined effects of spatially variable flow and mineralogy on the attenuation of acid mine drainage in groundwater. Appl Geochem 23:1419–1436. doi:10.1016/j.apgeochem.2007.12.029

Martín-Vide JP, Ferrer-Boix C, Ollero A (2010) Incision due to gravel mining: modeling a case study from the Gállego River, Spain. Geomorphology 117:261–271. doi:10.1016/j.geomorph.2009.01.019

Mayes WM, Potter HAB, Jarvis AP (2010) Inventory of aquatic contaminant flux arising from historical metal mining in England and Wales. Sci Total Environ 408:3576–3583. doi:10.1016/j.scitotenv.2010.04.021

Miller JR (1997) The role of fluvial geomorphic processes in the dispersal of heavy metals from mine sites. J Geochemical Explor 58:101–118. doi:10.1016/S0375-6742(96)00073-8

Mongolian Ministry for Environment and Green Development (MEGD) (2012) Tuul River Basin integrated water resource management plan, MEGD, Ulanbaatar, Mongolia

Mol JH, Ouboter PE (2004) Downstream effects of erosion from small scale gold mining on the instream habitat and fish community of a small neotropical rainforest stream. Conserv Biol 18(1):201–214. doi:10.1111/j.1523-1739.2004.00080.x

Nogina NA (1990) Uniqueness of soils and soil-forming processes in the central Asian facies (taiga, steppe, desert). Soviet Soil Sci Soviet Soil Sci 22(3):1–11

Onda Y, Kato H, Tanaka Y, Tsujimura M, Davaa G, Oyunbaatar D (2007) Analysis of runoff generation and soil erosion processes by using environmental radionuclides in semiarid areas of Mongolia. J Hydrol 333(1):124–132. doi:10.1016/j.jhydrol.2006.07.030

Pietroń J, Chalov SR, Chalova AS, Alekseenko AV, Jarsjö J (2017) Extreme spatial variability in riverine sediment load inputs due to soil loss in surface mining areas of the Lake Baikal basin. Catena 152:82–93. doi:10.1016/j.catena.2017.01.008

Pietroń J, Jarsjö J, Romanchenko A, Chalov SR (2015) Model analyses of the contribution of in-channel processes to sediment concentration hysteresis loops. J Hydrol 527:576–589. doi:10.1016/j.jhydrol.2015.05.009

Qi Y, Liu J, Shi H, Hu Y, Zhuang D (2008) Using ^{137}Cs tracing technique to estimate wind erosion rates in the typical steppe region, northern Mongolian plateau. Chin Sci Bull 53(9):1423–1430. doi:10.1007/s11434-008-0070-6

Schiettecatte W, Cornelis WM, Acosta ML, Leal Z, Lauwers N, Almoza Y, Gabriels D (2008) Influence of landuse on soil erosion risk in the Cuyaguateje watershed (Cuba). Catena 74:1–12. doi:10.1016/j.catena.2007.12.003

Shi ZH, Ai L, Fang NF, Zhu HD (2012) Modeling the impacts of integrated small watershed management on soil erosion and sediment delivery: a case study in the Three Gorges area, China. J Hydrol 438:156–167. doi:10.1016/j.jhydrol.2012.03.016

Salminen R, Batista MJ, Bidovec M, Demetriades A, De Vivo B, De Vos W, Duris M, Gilucis A, Gregorauskiene V, Halavic J, Heitzmann P, Lima A, Jordan G, Klaver G, Klein P, Lis J, Locutura J, Marsina K, Mazreku A, O'Connor PJ, Olsson SA, Ottesen RT, Petersell V, Plant JA, Reeder S, Salpeteur I, Sandstrom H, Siewers U, Steenfelt A, Tarvainen T (2005) Geochemical atlas of Europe. Part 1: background information, methodology and maps. Geological Survey of Finland, Espoo, http://www.weppi.gtk.fi/publ/foregsatlas/index.php

Shacklette HT, Boerngen JG (1984) Element concentrations in soils and other surficial materials of the conterminous United States. US Geol. Surv. Prof. Paper 1270. http://www.pubs.usgs.gov/pp/1270/

Somprasong K, Chaiwiwatworakul P (2015) Estimation of potential cadmium contamination using an integrated RUSLE, GIS and remote sensing technique in a remote watershed area: a case study of the Mae Tao Basin. Thailand Environ Earth Sci 73(8):4805–4818. doi:10.1007/s12665-014-3766-8

Theuring P, Rode M, Behrens S, Kirchner G, Jha A (2013) Identification of fluvial sediment sources in a meso-scale catchment, northern Mongolia. Hydrol Process 27(6):845–856. doi:10.1002/hyp.9684

Theuring P, Collins AL, Rode M (2015) Source identification of fine-grained suspended sediment in the Kharaa River Basin, northern Mongolia. Sci Total Environ 526:77–87. doi:10.1016/j.scitotenv.2015.03.134

Thorslund J, Jarsjö J, Chalov SR, Belozerova EV (2012) Gold mining impact on riverine heavy metal transport in a sparsely monitored region: the upper Lake Baikal Basin case. J Environ Monit 14:2780–2792. doi:10.1039/c2em30643c

Thorslund J, Jarsjö J, Wällstedt T, Mörth CM, Lychagin MY, Chalov SR (2016) Speciation and hydrological transport of metals in a non-acidic river system: field data and model predictions. Reg Environ Change (this issue). doi:10.1007/s10113-016-0982-7

Törnqvist R, Jarsjö J, Karimov B (2011) Health risks from large-scale water pollution: trends in central Asia. Environ Int 37:435–442. doi:10.1016/j.envint.2010.11.006

Törnqvist R, Jarsjö J, Pietroń J, Bring A, Rogberg P, Asokan SM, Destouni G (2014) Evolution of the hydro-climate system in the Lake Baikal basin. J Hydrol 519:1953–1962. doi:10.1016/j.jhydrol.2014.09.074

USGS (2014) U.S. Geological Survey. Earth Explorer. [Online]: http://earthexplorer.usgs.gov/, Accessed Sep 2014 and May 2015.

Van der Knijff JM, Jones RJA, Montanarella L (2000) Soil erosion risk assessment in Europe. European Commission Directorate General, Joint Research Centre (JCR), Space Applications Institute, European Soil Bureau. http://www.unisdr.org/files/1581_ereurnew2.pdf

Van Oost K, Govers G, Desmet P (2000) Evaluating the effects of changes in landscape structure on soil erosion by water and tillage. Landsc Ecol 15(6):577–589. doi:10.1023/A:1008198215674

Van Rompaey A, Verstraeten G, Van Oost K, Govers G, Poesen J (2001) Modelling mean annual sediment yield using a distributed approach. Earth Surf Proc Land 26(11):1221–1236. doi:10.1002/esp.275

Verstraeten G, Prosser IP, Fogarty P (2007) Predicting the spatial patterns of hillslope sediment delivery to river channels in the Murrumbidgee catchment, Australia. J Hydrol 334(3):440–454. doi:10.1016/j.jhydrol.2006.10.025

Viers J, Dupré B, Gaillardet J (2009) Chemical composition of suspended sediments in world rivers: new insights from a new database. Sci Total Environ 407(2):853–868. doi:10.1016/j.scitotenv.2008.09.053

Visser A, Kroes J, van Vliet MT, Blenkinsop S, Fowler HJ, Broers HP (2012) Climate change impacts on the leaching of a heavy metal contamination in a small lowland catchment. J Contam Hydrol 127(1):47–64. doi:10.1016/j.jconhyd.2011.04.007

Walling DE, Fang D (2003) Recent trends in the suspended sediment loads of the world's rivers. Glob Planet Chang 39(1):111–126. doi:10.1016/S0921-8181(03)00020-1

Zhao G, Klik A, Mu X, Wang F, Gao P, Sun W (2015) Sediment yield estimation in a small watershed on the northern loess plateau, China. Geomorphology 241:343–352. doi:10.1016/j.geomorph.2015.04.020